



RESEARCH ARTICLE

CHARACTERIZATION OF ORGANOSILICA HYBRID MATERIALS DERIVED FROM  
TETRAETHYLORTHOSILANE (TEOS) AND VINYLTRIMETHOXYSILANE (VTES)  
WITH SOL-GEL METHOD

<sup>1</sup>Ahmed A. Abdel-Aal, \*,<sup>1</sup>Islam E. Soliman, <sup>1</sup>Amir A. Elhadad, <sup>2</sup>AbdAllah Mubarak and  
<sup>1</sup>Khairy T. Ereiba

<sup>1</sup>Biophysics Branch, Physics Department, Faculty of Science, Al-Azhar University, Nasr City 11884, Cairo, Egypt  
<sup>2</sup>Physics Department, Faculty of Science, Al-Azhar University, Nasr City 11884, Cairo, Egypt

ARTICLE INFO

Article History:

Received 17<sup>th</sup> June, 2016  
Received in revised form  
21<sup>st</sup> July, 2016  
Accepted 30<sup>th</sup> August, 2016  
Published online 20<sup>th</sup> September, 2016

Key words:

Biomaterials, Hybrid, In-vitro,  
SBF, Protein adsorption, Hydroxyapatite.

ABSTRACT

In this study, TEOS-VTES-CaCl<sub>2</sub> hybrids were synthesized via sol-gel method with different molar ratios (T0) VTES: TEOS1:0; (T1) VTES: TEOS1:1; (T2) VTES: TEOS1:2; (T3) VTES: TEOS 1:3 and, (T4) VTES: TEOS 1:4, respectively. Development of a calcium phosphate (CP) layer on their surfaces was studied by soaking them in a simulated body fluid (SBF). The consequent formation of the CP layer and structural discrepancies of the formed layer of various samples were studied by means of appropriate techniques such as X-ray diffractometry, Fourier transform infrared spectroscopy and scanning electron microscopy equipped with an energy dispersive system (EDS). It was found that the rate of *in-vitro* apatite formation on hybrid surface decreased with increasing the amount of TEOS precursor. For biomaterials application the best surface in terms of *in-vitro* bioactivity, adsorbed protein amounts and thermal stability is the T2 surface containing VTES: TEOS1:2.

Copyright©2016, Ahmed A. Abdel-Aal et al. This is an open access article distributed under the Creative Commons Attribution License, which permits unrestricted use, distribution, and reproduction in any medium, provided the original work is properly cited.

Citation: Ahmed A. Abdel-Aal, Islam E. Soliman, Amir A. Elhadad, AbdAllah Mubarak and Khairy T. Ereiba, 2016. "Characterization of Organosilica hybrid materials derived from Tetraethylorthosilane (TEOS) and Vinyltrimethoxysilane (VTES) with sol-gel method", *International Journal of Current Research*, 8, (09), 37647-37653.

INTRODUCTION

The application of bioactive ceramics such as Bioglass® (Hench *et al.*, 1971), glass-ceramic A-W (Kokubo *et al.*, 1982), and sintered hydroxyapatite (Jarcho *et al.*, 1977; Aoki *et al.*, 1977) are remains limited because of their brittleness and low flexibility. Bone is regarded as an organic-inorganic hybrid composed of hydroxyapatite and collagen fibers. Therefore, one of the important design features required of bioactive bone substitutes is of an organic-inorganic hybrid showing not only bone-bonding properties but also flexibility so as to achieve a lower Young's modulus than conventional bioactive ceramics. Recently, organic-inorganic hybrids with bone-bonding properties were proposed based on the fundamental understanding of the bone-bonding mechanisms of bioactive ceramics (Ohtsuki *et al.*, 2002; Ohtsuki *et al.*, 2007). Previous reports have already revealed that the essential requirement for artificial materials to show bone-bonding properties is the formation of a bone-like hydroxyapatite layer on their surface in

the body environment (Hench, 1991; Neo *et al.*, 1993). Hydroxyapatite formation ability can be evaluated *in-vitro* using a simulated body fluid (SBF) that has a composition similar in inorganic composition to body fluid, and formulated according to Kokubo *et al.* Previous research on the formation of hydroxyapatite layers on calcium silicate binary glasses in SBF has shown that hydroxyapatite formation was triggered not only by the release of calcium ions from the glass, but also by the formation of silanol (Si-OH) groups that may induce heterogeneous nucleation of hydroxyapatite on the glasses (Ohtsuki *et al.*, 1992; Li *et al.*, 1992). This means that organic modification of these chemical species, i.e., Si-OH and Ca<sup>2+</sup>, may lead to bioactive organic-inorganic hybrids. Therefore, the behavior of silanol groups is expected to have important contributions to determining not only the apatite formation on the organic-inorganic hybrid but also their mechanical strength. Hydrolysis and poly-condensation during the sol-gel processing are generally accelerated by the presence of catalysts such as HCl. Vinyltriethoxysilane (VTES) is a silane containing unsaturated double bonds with a reactive —OC<sub>2</sub>H<sub>5</sub> group that can combine with inorganic materials such as synthetic resins thus improving their performance by increasing their bond strength. Furthermore, the silane coupling agent which contains

\*Corresponding author: Islam E. Soliman,  
Biophysics Branch, Physics Department, Faculty of Science, Al-Azhar  
University, Nasr City 11884, Cairo, Egypt.

reactive vinyl groups at the side chain increases the possibility of polymerization with other reactive monomers. The aim of this work is to obtain tailor-made organic-inorganic hybrid with pre-designed bioactive properties. We hypothesized that the combination of inorganic (Tetraethyl orthosilicate TEOS) and organic (Vinyltriethoxysilane VTES) silane precursors at different molar ratios and incorporation of  $\text{Ca}^{2+}$  ions by mixing the TEOS/VTES hybrid with calcium salts such as ( $\text{CaCl}_2$ ) are expected to induce deposition of bioactive apatite in the Kokubo's simulated body fluid (SBF) which subsequently makes it applicable for bone regeneration.

## MATERIALS AND METHODS

### Samples preparation

VTES-TEOS hybrids were synthesized via sol-gel route by dissolving appropriate amounts of Vinyltriethoxysilane ((VTES;  $(\text{CH}_3\text{CH}_2\text{O})_3\text{SiCH}=\text{CH}_2$ , purchased from Alfa Aesar Company, Germany) and distilled water in ethanol (Merck). The VTES / EtOH /  $\text{H}_2\text{O}$  mixture was stirred for 15 minutes at room temperature. Then HCL (sigma aldrish Company, Canada) was added for acid hydrolysis to prevent phase separation. The VTES / EtOH /  $\text{H}_2\text{O}$  / HCL mixture was stirred for another 15 min at room temperature. Tetraethyl orthosilicate (TEOS;  $\text{Si}(\text{OC}_2\text{H}_5)_4$  purchased from sigma aldrish Company, Canada) was added to previous solution. Different molar ratios VTES: TEOS of (T0 (1:0), T1(1:1), T2(1:2), T3(1:3) and T4(1:4)) were proposed, Where the molar ratio of silane/water/ethanol of 1:3:3 was used. Mixture of VTES / EtOH /  $\text{H}_2\text{O}$  / HCL/ TEOS was stirred for 4 hours at room temperature. Finally 0.2 grams of  $\text{CaCl}_2$  (purchased from sigma aldrish Company, Canada) was added. The sol was stirred for 2 hours at  $60^\circ\text{C}$  to reach the sol-gel transition (Condensation process). The resulting gel was dried at  $120^\circ\text{C}$  in a drying oven for 6 days to obtain the prepared material in a xerogel form as shown in Figure (1). Finally the selected samples were crushed (milled) in an agate mortar and subject to different characterization techniques.

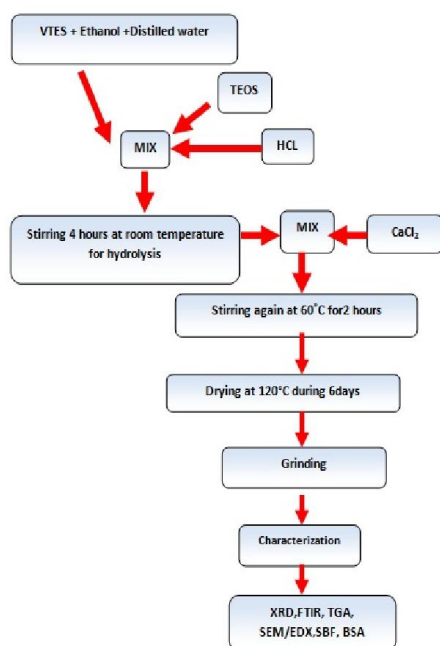


Fig. 1. Flow chart of VTES/TEOS preparation

## Characterization

### Thermogravimetric analysis (TGA)

Thermogravimetric analysis of the various VTES-TEOS- $\text{CaCl}_2$  organic-inorganic hybrids in xerogel form was performed on a SETARAM DTA-TG labsys™ Evolution-1750 equipment, with  $\alpha\text{-Al}_2\text{O}_3$  powders as a reference material. Samples of 5 mg crushed powder were put into an  $\text{Al}_2\text{O}_3$  crucible and the measurements were performed in the temperature range  $23\text{--}1000^\circ\text{C}$  (heating rate  $10^\circ\text{C}/\text{min}$ ) in air.

### X-ray diffraction (XRD)

The phase analysis of the samples was examined by X-ray diffractometer, model BRUKER Germany, D8 ADVANCE using monochromatic  $\text{Cu K}\alpha$  radiation ( $\lambda = 0.15406\text{ nm}$ ), scanning rate  $0.1^\circ$  in the  $2\theta$  ranging from  $10^\circ$  to  $100^\circ$  step time 1 sec. at 40 kV and 40 mA.

### Attenuated total Reflectance infrared spectroscopy (FT-IR)

ATR-FTIR absorption spectra were recorded at room temperature in the  $400\text{--}4000\text{ cm}^{-1}$  range with a resolution of  $4\text{ cm}^{-1}$  at room temperature using a spectrometer of type (FT-IR-400, JASCO, Japan). Each sample was prepared according to standard procedure by mixing about 2.00 mg of powder sample with 200 mg of KBr, which was subsequently pressed into pellet in an evacuated die. A background reading was taken before collecting spectra from the samples and was subtracted from the sample spectra.

### Scanning electron microscope (SEM)

The surface morphology of the resultant hybrids before and after immersion in SBF was performed by using Philips XL 30 scanning electron microscope (SEM) with an accelerating voltage of 30 kV. Specimens were placed on a stub using a carbon sticker and examined under the microscope. For chemical analysis, the samples were examined in energy dispersive X-ray analysis coupled to the SEM instrument (EDXA;  $30\text{ mm}^2\text{ Si (Li) R-RSUTW}$  detector) at 15 kV acceleration voltages. EDX used to compare the intensities of calcium (Ca), phosphorus (P) in the resultant hybrids before and after immersion in SBF.

### In-vitro assay

#### a) Simulated body fluid (SBF)

The *in-vitro* bioactivity of the prepared VTES-TEOS- $\text{CaCl}_2$  hybrids was tested by soaking in 50 ml of Kokubo's simulated body fluid (SBF) (Kokubo *et al.*, 1982). The pH of the SBF solution was buffered at 7.4. The specimens within plastic containers were immersed in a thermodynamic (shaking-water bath at constant separate then incubated for 33 days at  $37^\circ\text{C}$ . After 33 days of immersion, the specimens were removed from the solution, rinsed with distilled water and left to dry at room temperature.

#### b) Protein adsorption

To study the physiological behavior of the Organic-inorganic samples, protein adsorption onto these surfaces was studied. Bovine serum albumin (BSA) was used as representative

protein. 0.2 gm of bovine serum albumin was added to 200 ml of PBS (Dissolve 8g of NaCl, 0.2g of KCl, 1.805g  $\text{Na}_2\text{HPO}_4 \cdot 2\text{H}_2\text{O}$  and 0.30717g  $\text{K}_2\text{HPO}_4$  in 800 ml distilled  $\text{H}_2\text{O}$ . Adjust pH to 7.4 with HCl. Adjust volume to 1L with additional distilled  $\text{H}_2\text{O}$ ) at pH 7.4 and  $37^\circ\text{C}$ . 4 gm of each sample was added to 40 ml of the previous mixture. Adsorption was allowed to proceed in an incubator for 1 h at  $37^\circ\text{C}$ . Upon completion of adsorption, the samples were thoroughly rinsed with PBS 3 times and with water to remove unbound proteins (non-adsorbed) and salt residues then dried at  $37^\circ\text{C}$ . Protein adsorption on the surface of the samples was determined by using FTIR technique.

## RESULTS AND DISCUSSION

### Thermal gravimetric analysis (TGA):

Figure (2): Shows TGA curves ( $25\text{-}1000^\circ\text{C}$  temperature range) of VTES-TEOS- $\text{CaCl}_2$  hybrid as a function of TEOS content. In order to follow some significant effects, the weight loss was studied in three temperature intervals:  $0\text{-}145^\circ\text{C}$  (I),  $145\text{-}400^\circ\text{C}$  (II),  $400\text{-}600^\circ\text{C}$  (III).

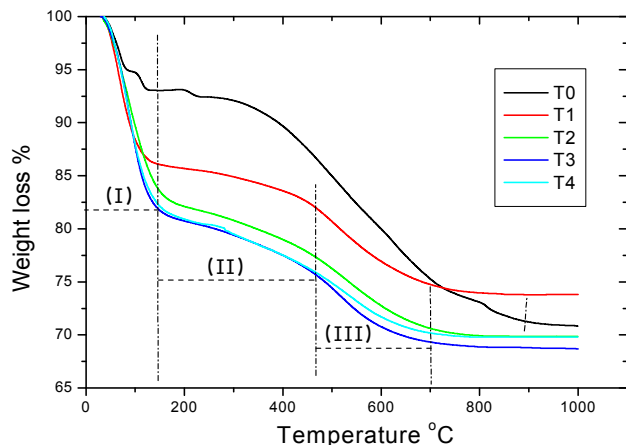


Fig. 2. TGA curves of pure VTES - $\text{CaCl}_2$  hybrid without TEOS, and mixed VTES-TEOS- $\text{CaCl}_2$  hybrids as a function of TEOS content

**The initial weight loss (Region I)**, in all these samples, is considered to be the result of the elimination of the condensation by-products, ethanol and water (Park *et al.*, 2009). Quantity of water and ethanol that samples are losing, increases with the decreasing of hydrocarbon chain (where TEOS content increases). This fact agrees with the more susceptibility to hydrolysis in the case of increasing the inorganic content of the system (TEOS).

**The second weight loss (Region II)**, is due to the partial thermal degradation of organic matter in hybrids. The elimination of organic matter in pure VTES- $\text{CaCl}_2$  sample (T0) occurs from  $145$  up to  $946^\circ\text{C}$  (22.14% weight loss), whereas in the VTES-TEOS hybrids, this loss starts from  $145^\circ\text{C}$  to  $466^\circ\text{C}$ . (3.97%, 6.33%, 6.14%, 6.42% for T1, T2, T3, T4). The elimination of organic components from the hybrids start at  $150^\circ\text{C}$ , this indicates that, in order to avoid the elimination of organics from the VTES - TEOS -  $\text{CaCl}_2$  hybrid, the hybrid should be cured while being prepared at a temperature which

does not exceeds  $150^\circ\text{C}$ . In other words,  $120^\circ\text{C}$  is a suitable temperature for curing these hybrids.

**The third weight loss stage (Region III)** at  $466\text{-}700^\circ\text{C}$  is due to the complete burning of organics in the hybrid (Jing and Hou, 2007). The TGA curves became flat at  $700\text{-}1000^\circ\text{C}$  because the organic component had been completely removed, leaving behind only an inorganic components as  $\text{SiO}_2$  and  $\text{CaCl}_2$ .

### X-ray Diffraction (XRD):

Figure (3): shows the XRD patterns of pure VTES- $\text{CaCl}_2$  (T0) and mixed TEOS-VTES- $\text{CaCl}_2$  (T1-T4) hybrid xerogel powder.

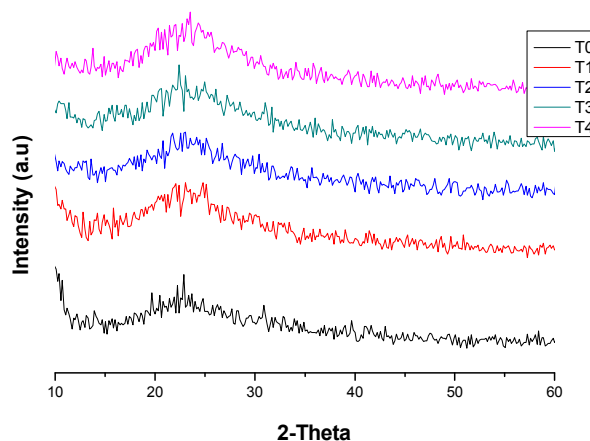


Fig. 3. XRD patterns of pure VTES- $\text{CaCl}_2$  and VTES-TEOS- $\text{CaCl}_2$  hybrid as a function of TEOS content

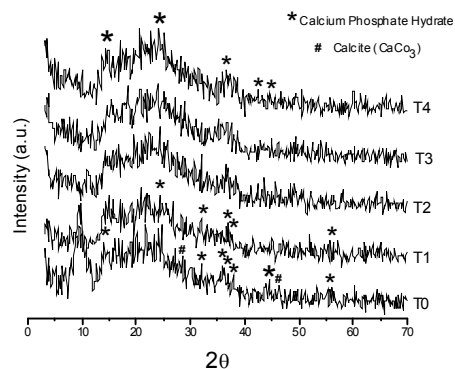


Fig (4): XRD patterns of pure VTES- $\text{CaCl}_2$  (T0) and Mixed TEOS-VTES- $\text{CaCl}_2$  hybrids T1, T2, T3 and T4 after immersion in SBF for 30 days.

Figure (4): shows the XRD patterns of pure VTES-  $\text{CaCl}_2$  and TEOS-VTES-  $\text{CaCl}_2$  hybrid sol-gel after immersion in SBF. From the figure, it could be observed that, some crystalline peaks appear in the XRD patterns, indicating the formation of a crystalline layer on the surface of the samples. Initially, two well-defined hydroxyl apatite (HA) peaks develop at  $2\theta$  values of  $2\theta=31.8^\circ$  (211) and  $25.8^\circ$  (002) according to the standard JCPDS cards (76-0694), Wide diffraction peak at angles ( $2\theta$ ) at  $32.18^\circ$ ,  $34.8^\circ$  corresponds to the overlapping of (1 1 2), (3 0 0) reflections planes of the well- crystallized HA. That the main developed phase is HA with minor traces of Calcite phase.

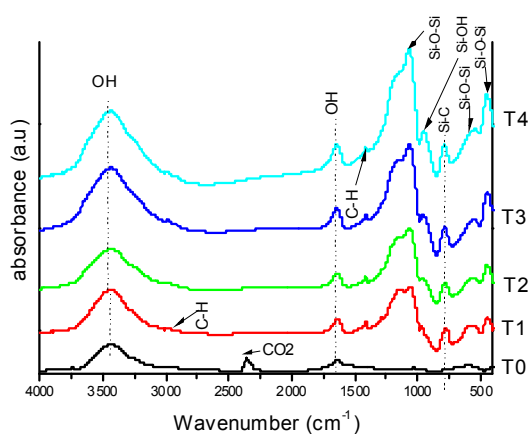


Fig. (5) FTIR absorption spectra of pure VTES-CaCl<sub>2</sub> (T0) and Mixed TEOS-VTES-CaCl<sub>2</sub> systems with different molar ratios (T0) VTES: TEOS1:0; (T1) VTES: TEOS1:1; (T2) VTES: TEOS1:2; (T3) VTES: TEOS 1:3 and, (T4) VTES: TEOS 1:4, respectively.

Characteristic peaks of apatite were observed in the patterns of all specimens with higher peak intensity for control sample T0, but intensity of apatite peaks decreased in T1 up to T4 sample, Figure (4). From the XRD patterns it was found that the rate of *in-vitro* apatite formation on hybrid surface decreased with increasing the amount of TEOS precursor.

#### Fourier transforms infrared spectroscopy (FTIR)

The main regions in FTIR spectra of mixed VTES-TEOS-CaCl<sub>2</sub> hybrids are shown in Figure (5) (curves T1-T4). For comparison, FTIR spectrum of a pure VTES-CaCl<sub>2</sub> xerogel without TEOS, S0 (curve T0) is also displayed. In the spectrum of pure VTES -CaCl<sub>2</sub> hybrid without TEOS, T0, Figure (5) the bands observed at 3431 cm<sup>-1</sup> is originate from O-H band stretching and bending of H<sub>2</sub>O adsorbed molecular water (Glaser and Wilkes, 1988). The absorbance bands at 2924 cm<sup>-1</sup> are attributed to stretching vibrations of C-H bonds (Glaser and Wilkes, 1988). The bands at 1638 cm<sup>-1</sup>(O-H), and 1408 cm<sup>-1</sup>(C-H) are characteristics bands of in the (Si-C=C) group of VTES (Glaser and Wilkes, 1988; Franquet *et al.*, 2003). The spectrum shows other bands at 2360 cm<sup>-1</sup> (attributed to absorption by the atmospheric CO<sub>2</sub>), 1026-1137 cm<sup>-1</sup> (Si-O-Si), 663 and 773 cm<sup>-1</sup> (Si-C).the bands at 460,552cm<sup>-1</sup> are assigned to Si-O-Si (El hadad *et al.*, 2011). For the mixed VTES-TEOS-CaCl<sub>2</sub> hybrids with different TEOS: VTES molar ratios, All hybrids present a characteristic band around 1026-1198 cm<sup>-1</sup> attributed to Si-O-Si group stretching vibrations, which are It is clear that, as the TEOS:VTES ratio increases (curves T1 and T4), characteristic vibration bands of siloxane bands groups increase, at 1026-1198 cm<sup>-1</sup>, that are assigned to Si-O-Si. Besides, in mixed TEOS-VTES-CaCl<sub>2</sub> xerogels, one weak band at 940 cm<sup>-1</sup>, which can be assigned to  $\nu$  Si-O of silanol groups (Si-OH) of TEOS and VTES, also appear. Figure (6) shows the FTIR spectra for hybrids after soaking in SBF for 30 days. For all samples Figure (6) the bands appeared in the range 800–1100 cm<sup>-1</sup> are ascribed to the stretching modes of SiO<sub>4</sub> tetrahedra. The wide absorption band at 1000–1100cm<sup>-1</sup> assigned to the asymmetric stretching mode Si-O-Si (asym), the one weak band around 788cm<sup>-1</sup> is associated to symmetric stretching vibration Si-O-Si (sym). Furthermore, the band observed at 450cm<sup>-1</sup> is attributed to bending mode of Si-O-Si that shifted to high wave number in spectra of hybrid samples

(Glaser and Wilkes, 1988). The small shoulder observed at 775 cm<sup>-1</sup> ( $\nu_2$ ) and the weak peak at 1411 cm<sup>-1</sup> ( $\nu_3$ ) are the indications of the presence of CO<sub>3</sub><sup>2-</sup> groups in the lattice of HA (Li *et al.*, 1992). Intensity of these bands decreased from T0 up to T4 corresponding to the behavior of HA. The C-H alkyl stretching band can be observed at 2000-2500 cm<sup>-1</sup> (Franquet *et al.*, 2003). 1535 cm<sup>-1</sup> may be attributed to the stretching vibration of C = C and C-O of the remaining non-hydrolyzed group of VTES precursor. 1111 cm<sup>-1</sup> is attributed to PO<sub>4</sub><sup>3-</sup> (Rodriguez *et al.*, 1999; Abdelmouleha *et al.*, 2007). Peaks at 560 cm<sup>-1</sup> are associated with the P-O bending mode of crystalline phosphate (apatite) formed on the samples surface. it was noted that this band appeared clearly in T0 and T1, but decreased gradually up to T4. Two bands located at 1653 and 3548 cm<sup>-1</sup>. These absorptions are characteristic of the presence of water related to the hygroscopic feature of the formed apatite. These results showed that the bioactivity of hybrid samples decreased as VTES amount decreased and TEOS increased (Glaser and Wilkes, 1988; Franquet *et al.*, 2003).

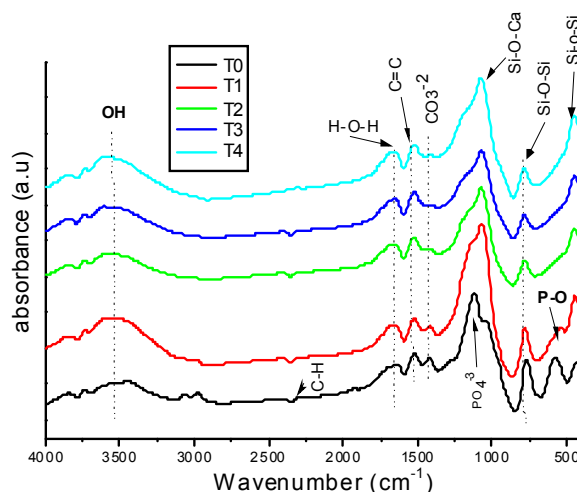


Fig.(6) FTIR absorption spectra of pure VTES -CaCl<sub>2</sub> (T0) and Mixed TEOS-VTES-CaCl<sub>2</sub> systems with different molar ratios (T0) VTES:TEOS 1:0 ; (T1) VTES:TEOS 1:1 ; (T2) VTES:TEOS 1:2 ; (T3) VTES:TEOS 1:3 and, (T4) VTES:TEOS 1:4, respectively after immersion in SBF.

#### Scanning Electron Microscope (SEM-EDX)

The surface morphology of the (T0, T2 and T4) samples before immersion in SBF is shown in Figure (7). The surfaces are rough /porous which could be attributed to the evaporation of ethanol and water during the curing step (120°C / 6 days). This pores/roughness could be useful during the *in-vitro* test, as these pores could act as nucleating sites and/or increasing the reaction rate by increasing the area of contact with the physiological fluids. On one hand, such surfaces could be useful for the bone-like apatite precipitations while being immersed in simulated body fluid (SBF) (Yang Kong *et al.*, 2007; Woo *et al.*, 2007).

#### The surface morphology and EDX analysis of the T0, T2 and T4 hybrids after 30 days of immersion in SBF is shown Figure 8

After 30 days of immersion in SBF, the surface of T0 sample is completely covered with apatite precipitations (Figure 8) due to

that the surface of T0 has some roughness features which could provide high surface area for reaction with SBF solution. The corresponding EDX spectra show that the main composition of formed surface layer was calcium and phosphorus. Even, being EDX a semi-quantitative analysis, these molar ratios indicates that the precipitates formed after SBF exposures should be apatite-like. The peaks corresponding to sodium and chloride are due to the presence of those elements in the SBF. The human bone also includes these elements, but is mainly made of apatite phase. The surface morphology of the sample T2 after immersion in SBF for 30 days is shown in Figure (8).

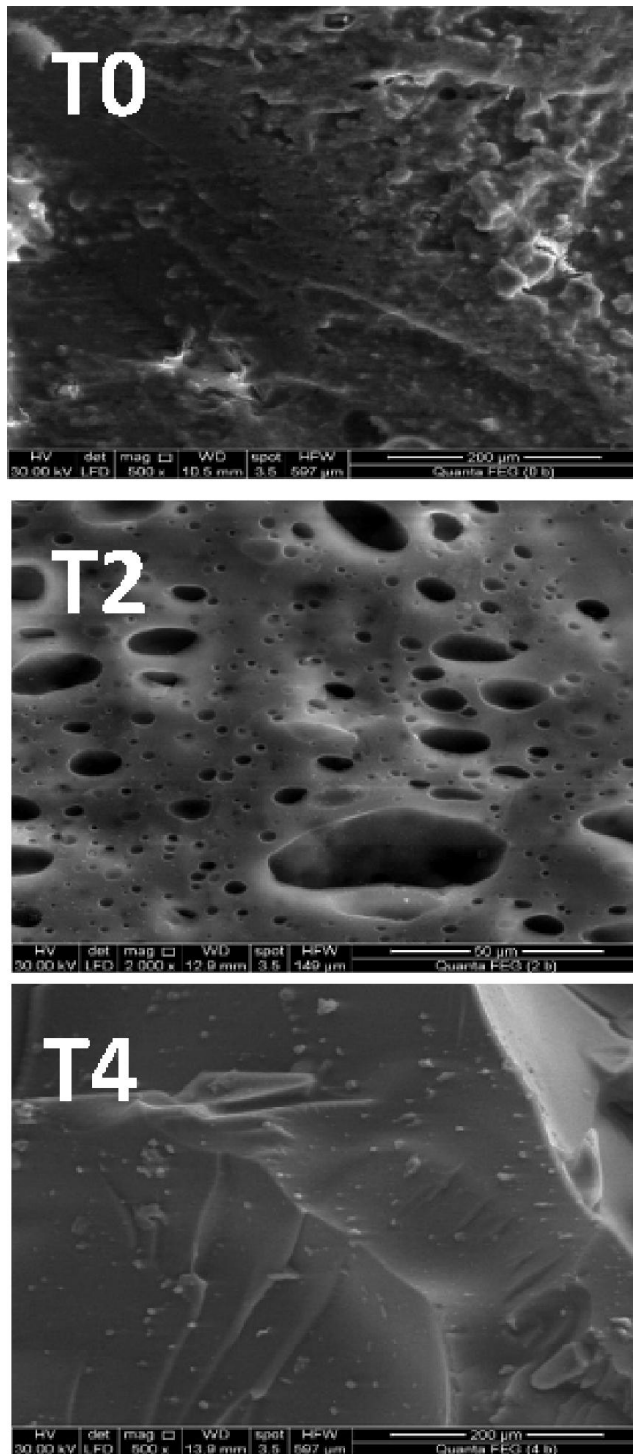


Fig. 7. SEM micrographs of the surface of the T0, T2 and T4 sample before immersion in SBF

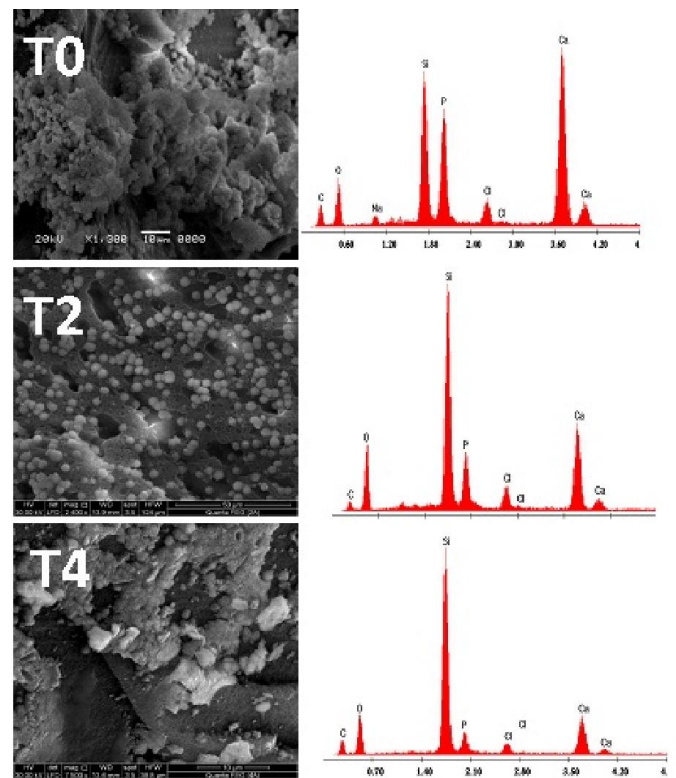


Fig. 8. SEM micrographs and EDX spectra of the surface of the T0, T2 and T4 hybrids after immersion in SBF

The surface is covered with less precipitation of apatite-like "non-well developed apatite" than T0. Because the surface of T2 has less roughness features than of that T0. Despite the elemental analysis obtained by EDX analysis, the peaks corresponding to the main components of apatite (Ca, P and O) were identified (Figure 4), with a Ca/P ratio of 1.48 ascribed to amorphous non-well developed apatite (Yang Kong *et al.*, 2007). The spectrum also exhibited peaks corresponding to Cl, which are due to the presence of this element in the SBF. The surface morphology of the sample T4 after immersion in SBF for 30 days is shown in Figure (8). The surface of T4 sample is partially covered with apatite precipitations less than T0 and T2. Due to the less roughness features. Also, The EDX analysis indicates that these precipitates have a Ca/P molar ratio that 1.54 and indicates the precipitation of apatite-like.

### Protein adsorption

The chemical composition and surface charge of biomaterial surfaces strongly affect the protein adsorption behavior (Woo *et al.*, 2007). This is perhaps through interaction between the functional groups on the samples surface and those of the protein itself. After immersion of the samples in 1 mg/mL Bovine Serum albumin solution in PBS, adsorption was allowed to proceed in an incubator for 1 h at 37 °C. The Amide I and Amide II bands in sample T2 are shown in Figure (9). There was an increase in the ratio of the Amide I to the Amide II on all the surfaces due to protein adsorption. The biggest increase in the Amide I/Amide II ratio was seen on T0 (1.01), then this ratio decreases gradually from T1 to T4 (1.008, 0.9828, 0.99, 0.969). According to the popularly accepted understanding, electrostatic interactions are very important for protein adsorption (Healy and Ducheyne, 1992).

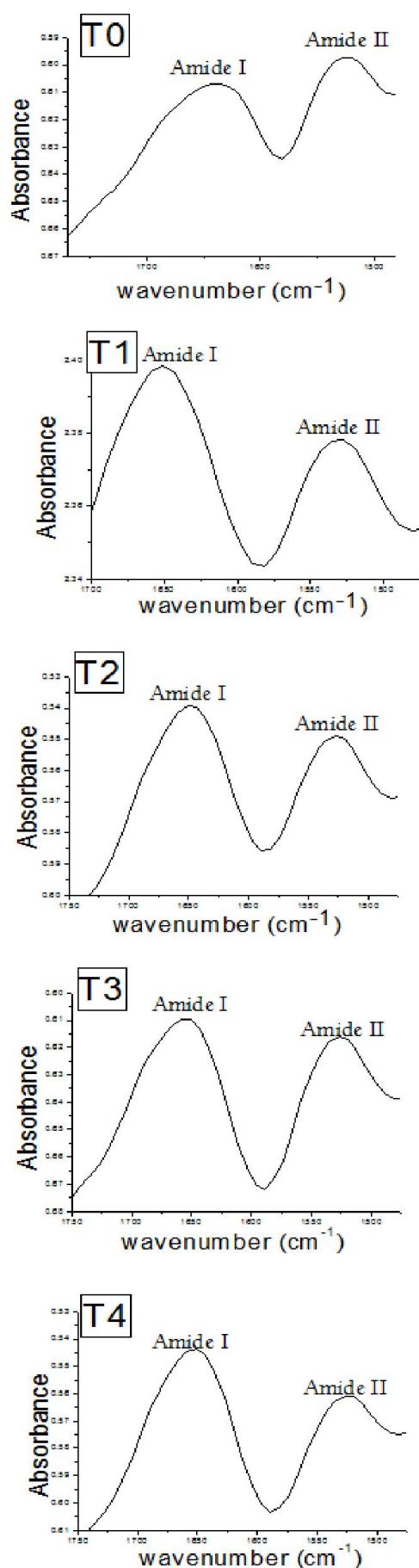


Fig. 9. Representative FTIR absorption spectra of all samples after immersion for 1 hour in BBS

The increase in the albumin adhesion on the surface of VTES-TEOS-CaCl<sub>2</sub> was likely due to the protein positive charge at pH 7.4. For Pure HAp, It has been reported that the protein adsorption on HAp is electrostatic in nature and two possible adsorption sites are involved and act as adsorption sites (Healy and Ducheyne, 1992). Thus in the HAp exist two sites where proteins bind to apatite. These two sites, positively charged surfaces (Ca sites, Ca<sup>2+</sup>) on HAp which can absorb negatively charged proteins and negative charged sites (P sites, PO<sub>4</sub><sup>3-</sup>) which can absorb positively charged proteins (Healy and Ducheyne, 1992). Amount of albumin have been adsorbed on the prepared hybrid samples as a result of the presence of, positively charged Ca<sup>2+</sup> ions. That, it could be concluded that the existence of Ca<sup>2+</sup> in the hybrid samples enhance its efficiency for protein adsorption. The variation of the adsorbed amounts could be resulted from the surfaces goes negative as the amounts of TEOS in the samples increase. Such precursors after hydrolysis-condensation processes make the surface more negative as a result of abundant Si-O<sup>-</sup> bonds.

### Conclusion

TEOS-VTES-CaCl<sub>2</sub> hybrids were synthesized via sol-gel method and development of a calcium phosphate (CP) layer on their surfaces was studied by soaking them in a simulated body fluid (SBF). The rate of *in-vitro* apatite formation on hybrid surface decreased with increasing the amount of TEOS precursor. The surface morphology of the sample T2 after immersion in SBF for 30 days covered with less precipitation of apatite-like "non-well developed apatite" than T0. These results showed that the best surface in terms of *in-vitro* bioactivity is the surface of T0 covered with well-developed bone-like apatite. The best surface in terms of bioactivity/thermal stability is the surface of the T2 surface as it contain the both organic and inorganic precursors which both essential for thermal stability as well as bioactivity. For biomaterials application the best surface in terms of *in-vitro* bioactivity, adsorbed protein amounts and thermal stability is the T2 surface containing VTES: TEOS /1:2.

### REFERENCES

- A. A. El hadad, Diogenes Carbonell, Violeta Barranco, Antonia Jiménez-Morales, Blanca Casal, Juan Carlos Galván, 2011. *ColloidPolymSci*, 289:1875–1883.
- Abdelmouleha M., Boufia S., Belgacemb MN., Dufresne A., 2007. *Compos. SciTechnol* 67:1627.
- Aoki H., Kato K., Ogiso M. and Tabata T. 1977. Sintered Hydroxyapatite as a New Dental Implant Materials, *J. Dent. Outlook*, 49: 567-575.
- Castillo S. J., Acosta M. C., Zayas MA. 2010. "Formation of ZnO in or on glasses by using the Sol-Gel and Chemical Bath Deposition Techniques", "Seas Transactions On Circuits and Systems", Issue 3, Vol 9.
- Franquet A., Terryn H., Vereecken J. 2003. *Appl Surf Sci* 211:259.
- Glaser RH. and Wilkes GL. 1988. *Polym Bull* 19:51.
- Healy KE. and Ducheyne P. 1992. Hydration and preferential molecular adsorption on titanium in vitro. *Biomaterials*, 13:553–61.
- Hench L.L. 1991. Bioceramics: From Concept to Clinic, *J. Am. Ceram. Soc.*, 74(7): 1487-1510.9. (1991).

- Hench L.L., Splinter R.J., Allen W.C. and Greenlee T.K. 1971. Bonding Mechanisms at the Interface of Ceramic Prosthetic Materials, *J. Biomed. Mater. Res. Symp.*, 2 (Part 1): 117-141.
- Jarcho M., Kay J.F., Gumaer K.I., Doremus R.H. and Drobeck H.P. 1977. Tissue, Cellular and Subcellular Events at a Bone-Ceramic Hydroxyapatite Interface, *J. Bioeng.*, 1: 79-92.
- Jing CB. and Hou JX. 2007. Sol-gel-derived alumina/polyvinylpyrrolidone hybrid nanocomposite film on metal for corrosion resistance, *J Appl Polym Sci.*, 105(2):697-705.
- Kokubo T., Shigematsu M., Nagashima Y., Tashiro M., Nakamura T., Yamamuro T. and Higashi S. 1982. Apatite- and Wollastonite-Containing Glass-Ceramics for Prosthetic Application, *Bull. Inst. Chem. Res., Kyoto Univ.*, 60: 260-268.
- Li, P.J., Ohtsuki C., Kokubo T., Nakanishi K., Soga N., Nakamura T. and Yamamuro T. 1992. Apatite Formation Induced by Silica Gel in a Simulated Body Fluid, *J. Am. Ceram. Soc.*, 75: 2094-2097.
- Neo, M., Nakamura T., Ohtsuki C., Kokubo T. and Yamamuro T. 1993. Apatite Formation on Three Kinds of Bioactive Material at an Early Stage in vivo: A Comparative Study by Transmission Electron Microscopy, *J. Biomed. Mater. Res.*, 27: 999-1006.
- Ohtsuki C., Miyazaki T. and Tanihara M. 2002. Development of Bioactive Organic-inorganic Hybrid for Bone Substitutes, *Mater. Sci. Eng.: C*, 22(1): 27-34.
- Ohtsuki C., Miyazaki T., Kamitakahara M. and Tanihara M. 2007. Design of Novel Bioactive Materials through Organic Modification of Calcium Silicate, *J. Euro. Ceram. Soc.*, 27: 1527-1533.
- Ohtsuki, C., Kokubo, T. and Yamamuro, T. 1992. Mechanism of Apatite Formation on CaO-SiO<sub>2</sub>-P<sub>2</sub>O<sub>5</sub> Glasses in a Simulated Body Fluid, *J. Non-Cryst. Solids*, 143: 84-92.
- Park HY., Kang DP., Na MK., Lee HW., Lee HH., Shin, DS., 2009. *J. Electroceram* 22(1-3):309-314.
- Rodriguez MA., Liso MJ., Rubio F., Rubio J., Oteo JL. 1999. *J. Mater. Sci.* 34:3867.
- Woo KM., Seo J., Zhang R., Ma PX. 2007. Suppression of apoptosis by enhanced protein on polymer/hydroxyapatite composite scaffolds. *Biomaterials* 28:2622-30.
- Yang K., WEI J., Wang C., Li Y. 2007. A study on in vitro and in vivo bioactivity of nano hydroxyapatite/polymer biocomposite, *Chinese Science Bulletin*, Vol. 52 , no. 2 , 267-271.

\*\*\*\*\*